

Acoustic and exact elastic impedance variations during CO₂ injection at the CaMI.FRS

Yichuan Wang and Don Lawton
yichuan.wang1@ucalgary.ca

Abstract

Acoustic impedance (AI) and elastic impedance (EI) give direct connections to the mechanical and fluid-related properties of the CO₂ storage complex. However, evaluation of their subtle time-lapse (TL) variations is complicated by the scaling and low-frequency uncertainties, and the various EI definitions involve different approximations and do not represent an elastic property of the medium. To solve these issues, we perform accurate waveform calibration for TL seismic data, and apply a robust impedance-inversion approach based on calibration of seismic records by using the well-log data. We also use an exact expression of EI in a matrix form, which truly represents the intrinsic physical property and accurately describes P- and S-wave propagations at arbitrary incidence angles. The above approaches are applied to TL DAS VSP data from the Field Research Station CO₂ injection project in southern Alberta, Canada. TL impedance variations are observed within the CO₂ injection zone, which are interpreted as being related to the CO₂ injection.

Different EI measures

From the linearization of Zoeppritz equation, Connolly (1999) initially introduces EI as

$$EI = \rho V_p \left(\rho^{-4K \sin^2 \theta} V_p^{\tan^2 \theta} V_s^{-8K \sin^2 \theta} \right).$$

To resolve the dimensionality issue, a normalized EI was proposed:

$$NEI = \rho V_p \left[\left(\rho / \rho_0 \right)^{-4K \sin^2 \theta} \left(V_p / V_{p,0} \right)^{\tan^2 \theta} \left(V_s / V_{s,0} \right)^{-8K \sin^2 \theta} \right].$$

To address that reflectivity is integrated along nonphysical path of constant θ , a raypath EI such as by Santos and Tygel (2004) is

$$RI = \frac{\rho V_p}{\sqrt{1 - V_p^2 p^2}} \exp \left[-2(2 + \gamma) V_s^2 p^2 \right].$$

EI matrix

We use the EI matrix proposed by Morozov (2010) from Hooke's law:

$$\begin{pmatrix} \sigma_{zz} \\ \sigma_{zx} \end{pmatrix} = \begin{pmatrix} (\lambda + 2\mu) \partial_z & \lambda \partial_x \\ \mu \partial_x & \mu \partial_z \end{pmatrix} \begin{pmatrix} u_z \\ u_x \end{pmatrix}.$$

$\tilde{\mathbf{Z}} = - \begin{pmatrix} (\lambda + 2\mu) \partial_z & \lambda \partial_x \\ \mu \partial_x & \mu \partial_z \end{pmatrix}$ relating the displacement to stress is defined as the impedance matrix.

- Represent the intrinsic physical property
- Rigorously describe all cases of P/SV-wave propagation at arbitrary incidence angles

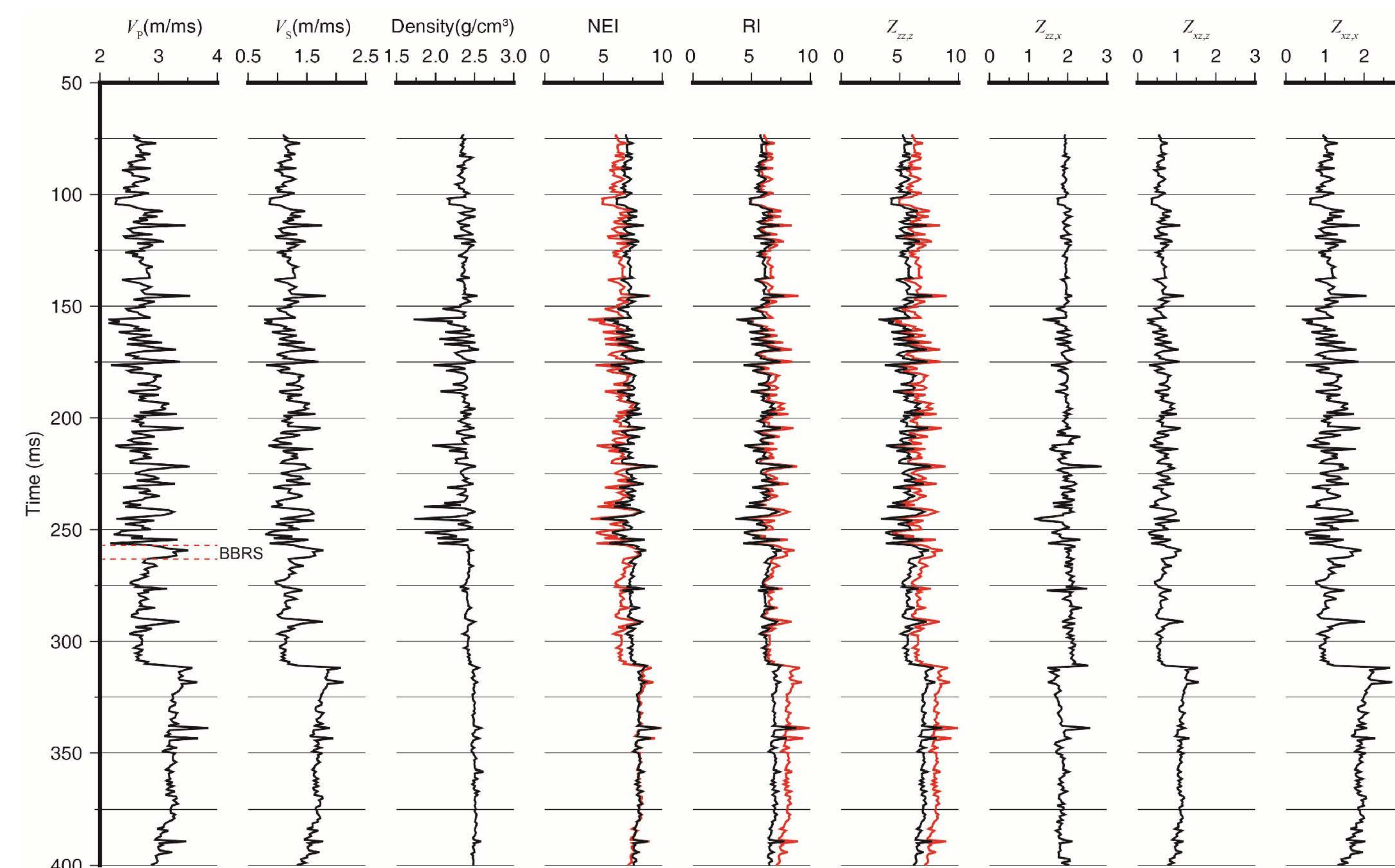
By considering a plane wave with the displacement $\exp[i(k \cos \theta z + k \sin \theta x - \omega t)]$, the conventional impedance matrix is

$$\mathbf{Z} = \frac{i}{\omega} \tilde{\mathbf{Z}} = \frac{k}{\omega} \begin{pmatrix} (\lambda + 2\mu) \cos \theta & \lambda \sin \theta \\ \mu \sin \theta & \mu \cos \theta \end{pmatrix}.$$

For the situation of incident P-wave, each component of impedance matrix \mathbf{Z} becomes

$$\begin{aligned} Z_{zz,z} &= \rho V_p \cos \theta, & Z_{zz,x} &= \rho V_p (1 - 2V_s^2/V_p^2) \sin \theta, \\ Z_{xz,z} &= \rho V_p (V_s^2/V_p^2) \sin \theta, & Z_{xz,x} &= \rho V_p (V_s^2/V_p^2) \cos \theta, \end{aligned}$$

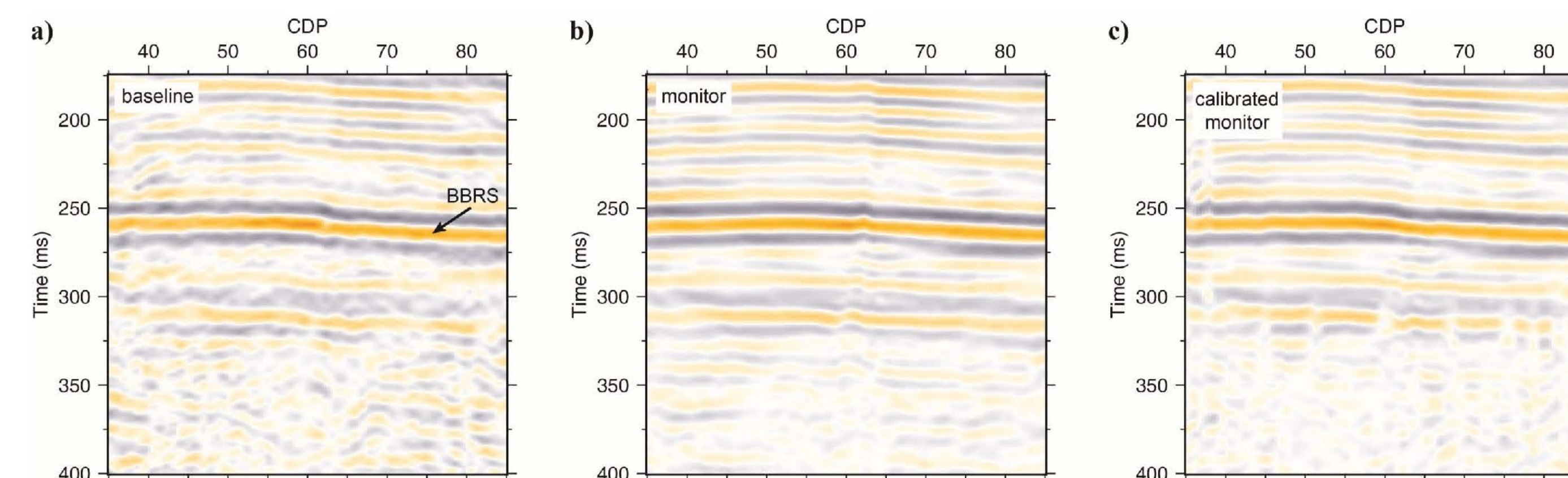
where the calculation reduces to the AI (ρV_p), and the V_s/V_p ratio from AVO inversion.



Velocity, density, NEI, RI and components of impedance matrix \mathbf{Z} at 30° incidence angle in the injection well from the FRS CO₂ injection project. The AI log is shown in red in NEI, RI, and $Z_{zz,z}$ for comparison. The CO₂ injection zone BBRs is indicated.

Waveform calibration

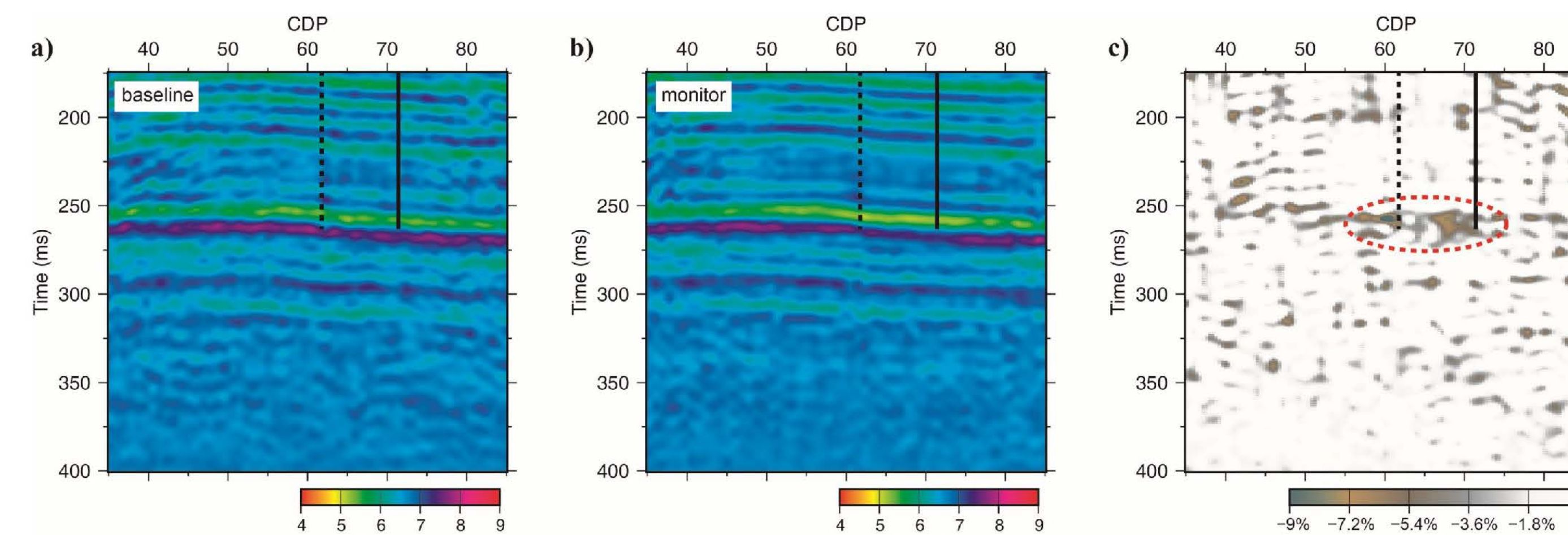
- Achieve accurate consistency of the records from different vintages while retaining the TL variations within the target zones
- Time shifting, amplitude corrections, and spectral shaping
- Similar to cross-equalization, but applied locally by time-variant linear filtering



Cross sections of a) baseline, b) monitor and c) calibrated monitor VSP CDP stack. The BBRs reflection is indicated.

AI inversion and TL variations

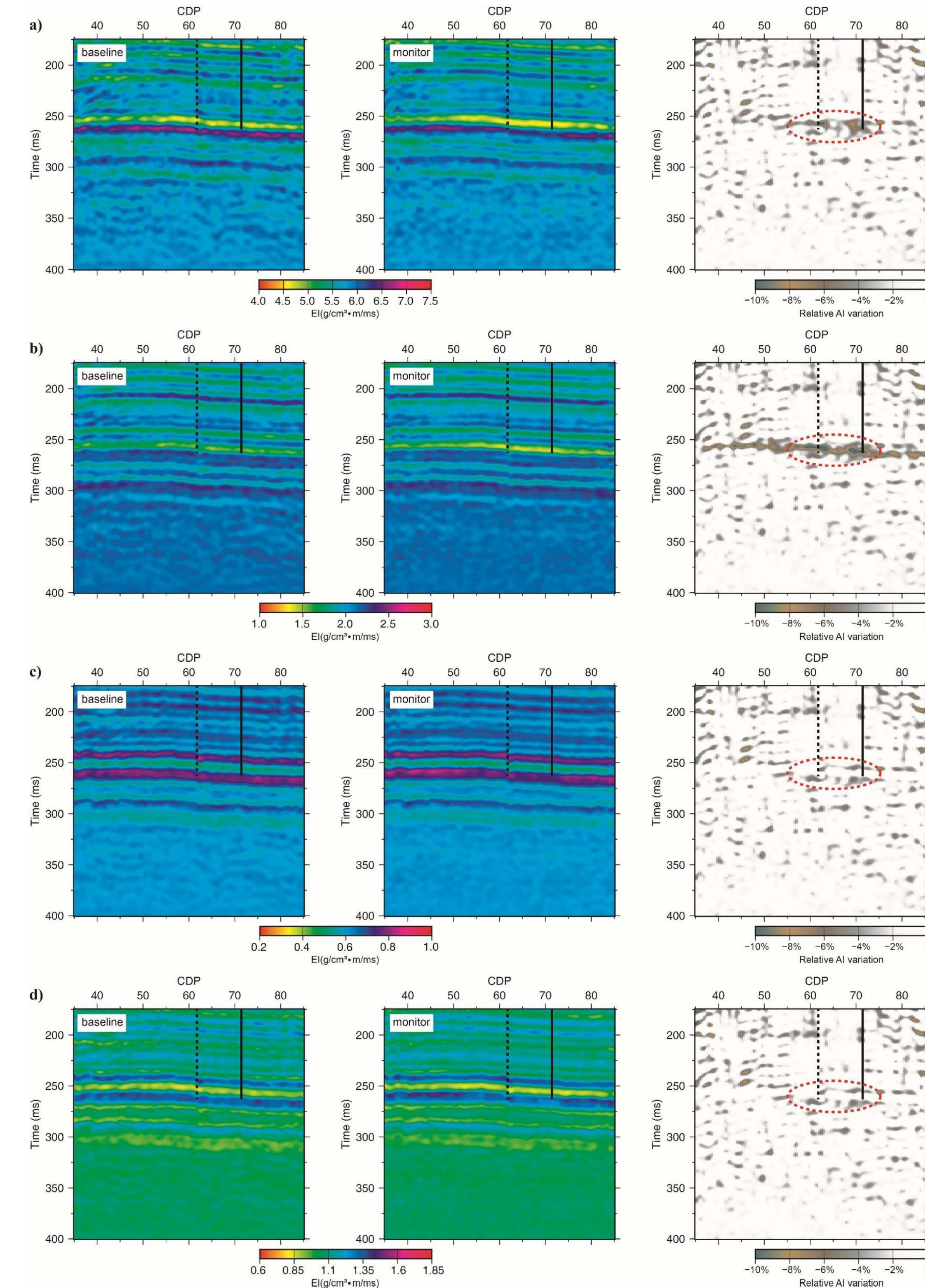
- The amplitude spectrum matches that of the well-log AI located near the imaging location
- Below the seismic frequency band, the AI also matches the one from well logs
- At each imaging location, the spatial pattern of reflectivity matches that of the seismic volume



Cross sections of a) baseline AI, b) monitor AI and c) relative AI variations. Dashed and solid black lines indicate observation well and injection well.

EI and TL variations

- All components of \mathbf{Z} are needed to accurately describe the reflection AVO effects
- 1D V_s/V_p ratio from well logs
- Decrease is stronger in $Z_{zz,x}$ than in $Z_{zz,z}$ or AI
- Less variations of $Z_{xz,z}$ and $Z_{xz,x}$ due to the increase of V_s/V_p ratio



Cross sections of baseline and monitor EI and their TL variations of components a) $Z_{zz,z}$, b) $Z_{zz,x}$, c) $Z_{xz,z}$, and d) $Z_{xz,x}$ of impedance matrix \mathbf{Z} at 30° incidence angle

References

Connolly, P., 1999, Elastic impedance: The Leading Edge, 18, 438–452.

Morozov, I. B., 2010, Exact elastic P/SV impedance: Geophysics, 75, no. 2, C7–C13.

Santos, L.T., and M.Tygel, 2004, Impedance-type approximations of the P-P elastic reflection coefficient: Modeling and AVO inversion: Geophysics, 69, 592–598.